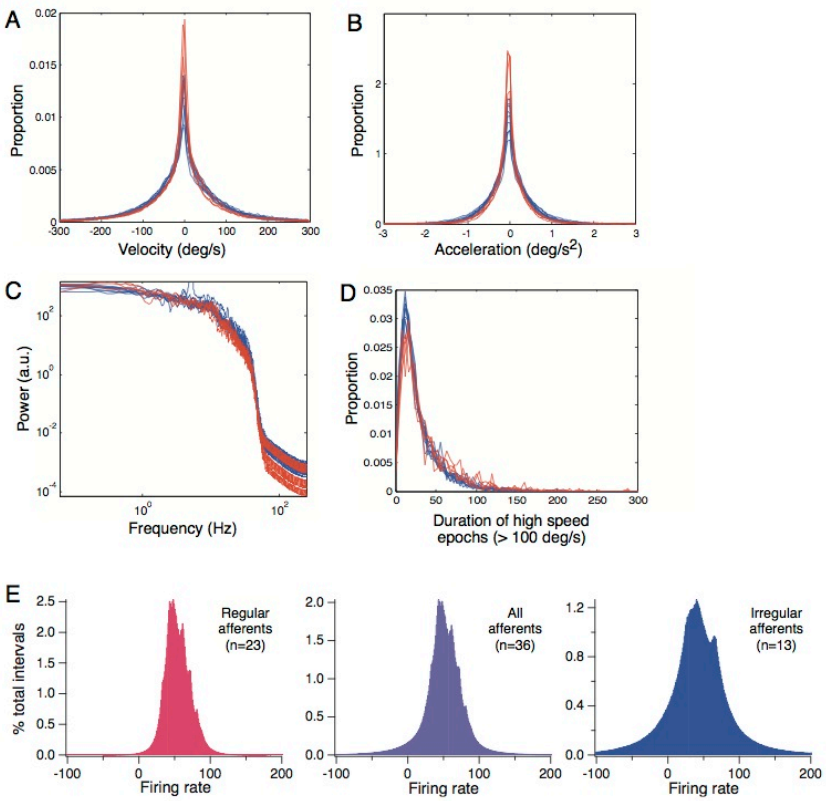

Figure S1, related to Figure 1. Statistics of mouse head movements and vestibular nerve afferent firing rates during unrestrained movement. Gyroscopic measurements of (A) head velocity and (B) acceleration, (C) spectral power, and (D) proportion of head movements epochs in which velocity exceeded 100 deg/s were obtained either with sensor mounted parallel to the skull surface (blue) or to the horizontal semicircular canal (red). Each trace represents data from one behavioral session consisting of 20 trials of recorded movement bouts between 10 and 20 sec duration. (E) Histograms of instantaneous firing rates of vestibular nerve afferents during natural movement in mice. Firing rates were calculated from 80 trials of 20 s movement epochs applied to the populations of regular and irregular afferents for which transfer functions were measured (Lasker et al, 2008). Firing rates during natural head movement range between 5 and 100 Hz for 98% of regular afferents (red), 75% of irregular afferents (blue) and 90% of the total population of afferents (purple).

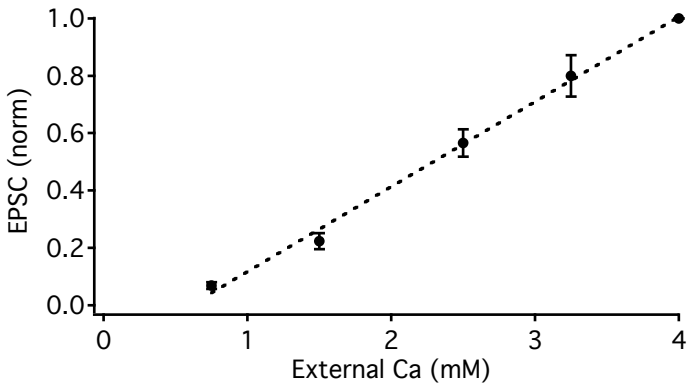

Figure S2, related to Figure 4. Ca2+-dependence of synaptic transmission in TEA. Peak EPSC amplitude was measured in TEA (1 mM) under 5 different release-probability conditions imposed by varying extracellular Ca2+ and Mg2+. EPSC amplitude increased linearly with respect to external Ca2+ (R^2= 0.99).

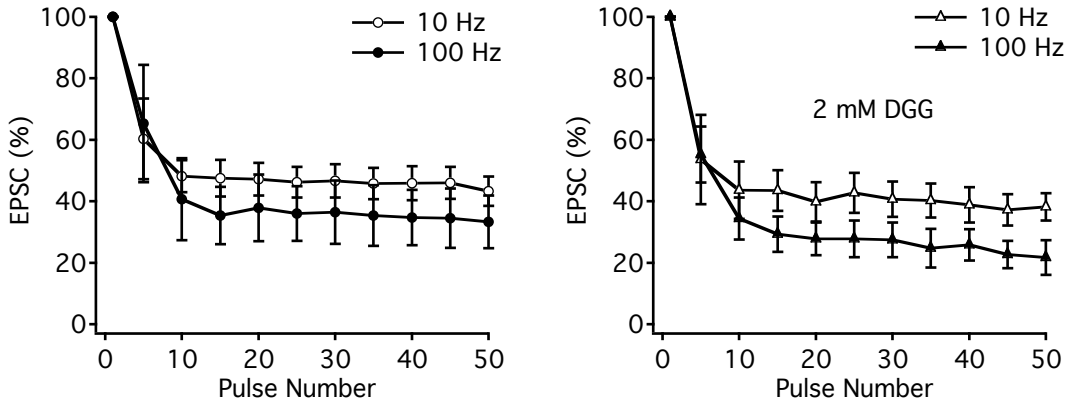

Figure S3, related to Figure 4. Changes in postsynaptic receptor sensitivity do not cause rate-dependent short-term depression in TEA. EPSC amplitude depressed more in response to 100 Hz than 10 Hz stimulation in 1 mM TEA ($SS_{100\ Hz}/SS_{10\ Hz} = 0.66 \pm 0.08$; left). Bath application of 2 mM γ-DGG (2 mM) did not restore rate-independent depression ($SS_{100\ Hz}/SS_{10\ Hz} = 0.69 \pm 0.10$, n=5; right). EPSCs are normalized to the first EPSC amplitude in each train.

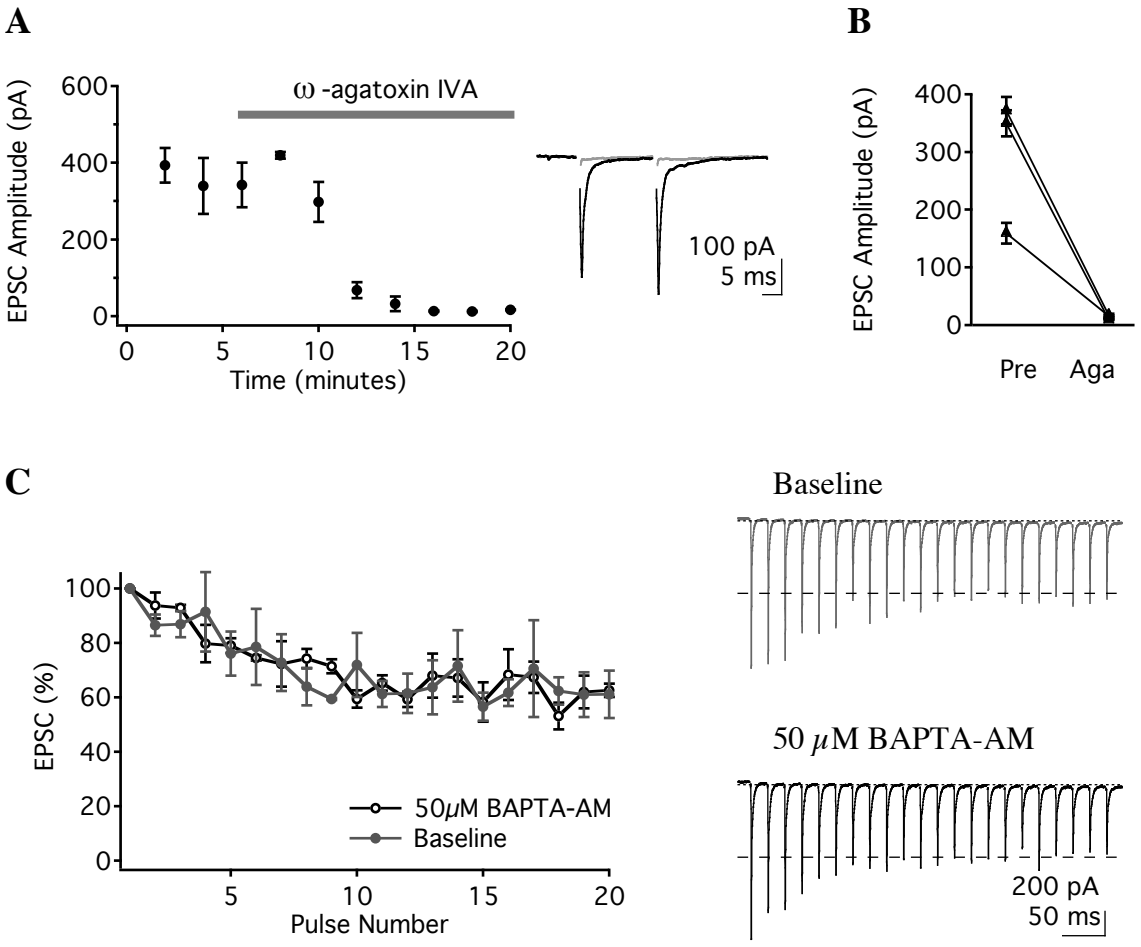

Figure S4, related to Figures 3 and 4. Vestibular nerve synaptic transmission depends on P/Q-type Ca2+ channels and is unaltered by externally applied BAPTA-AM. (A) Peak EPSC amplitude before and during the application of ω–agatoxin IVA (200 nM). (B) Effect of ω-agatoxin IVA application (n =3). (C) BAPTA-AM (50 μM) had no effect on short-term plasticity at vestibular nerve synapses. Group data (left) show BAPTA-AM application did not alter the short-term depression evoked by 50 Hz stimulation. Example EPSCs (right) recorded under baseline conditions (top) and >30 min following BAPTA-AM application (bottom).

Bouton	# Sections	Fiber Size	Volume (µm3)	# Release Sites	Release Site Surface Area (µm2)	Distance Nearest Neighboring Site (µm)
1	75	Large	20.85	14	0.23 ± 0.12	0.35 ± 0.22
2	51	Large	15.55	12	0.12 ± 0.05	0.56 ± 0.24
3	45	Large	7.19	10	0.07 ± 0.03	0.32 ± 0.16
4	69	Large	15.55	9	0.13 ± 0.07	0.49 ± 0.34
5	69	Small	17.95	16	0.14 ± 0.09	0.54 ± 0.33
6	69	Large	11.01	7	0.10 ± 0.02	0.86 ± 0.67
7	85	Large	17.33	23	0.32 ± 0.25	0.13 ± 0.10
8	86	Large	20.93	23	0.24 ± 0.19	0.15 ± 0.08

Table S1, related to Figure 2. Ultrastructural characteristics of vestibular nerve boutons from three-dimensional reconstructions of serial EM sections. Values indicate mean ± SD.

Supplemental Experimental Procedures

Head Motion Statistics

Surgery

3 mice were prepared for head movement measurements by chronically affixing a washer parallel to the skull. The mice were anesthetized with isoflurane, and 4-5 bone screws were implanted and covered with dental acrylic. The washer was placed on top of the screws, approximately parallel to the plane of the skull, and secured with dental acrylic. The mice were allowed to recover for several days after surgery.

Naturalistic head movements

At the beginning of each recording session, the mouse was briefly anesthetized with isoflurane, and the inertial sensor was affixed to the implanted washer with foam tape. The inertial sensor consisted of an analog MEMS yaw-rate gyroscope on a printed circuit board (modified ST Microelectronics LY550ALH evaluation board, 1.6g, 140 Hz bandwidth, +/- ~500 deg/s). Recordings were made in two configurations: (1) for "behavioral output" measurements the board was mounted parallel to the skull, and (2) for "vestibular input" measurements the board was placed on top of a balsa wood wedge (~30 degrees from the horizontal plane) to align the sensor with the horizontal semicircular canal. The mouse was placed on top of a flat platform (the top of its home cage) and allowed to explore, while the gyroscope output was sampled and digitized at 500 Hz (National Instruments USB-6009). These sessions typically consisted of stationary periods, locomotion, and/or exploratory head-movements. Trials in which grooming occurred were excluded from analysis. For the statistics in Supplemental Figure 1, only "non-stationary" epochs were considered for analysis. Non-stationary epochs were defined as continuous periods in which the instantaneous speed, low-pass filtered with a cutoff frequency of 3 Hz, exceeded 5 deg/s.

Processing of head movement traces

The published sensitivity value of the MEMS chip was verified by rotating it at known velocities using a servo-controlled rotation table. Voltages were converted to instantaneous velocity measurements by subtracting the baseline voltage and scaling by the gyroscope sensitivity (2 mV/deg/s). Because during the recording session the gyroscope would occasionally cut out, traces were inspected manually and such periods were removed from further analysis. The traces were then low-pass filtered in software with an 8^{th} order butterworth filter with cutoff frequency 40 Hz.

Conversion from head velocity to vestibular afferent firing rate

We simulated the firing patterns of semicircular canal afferent fibers using previously published transfer functions. We simulated the firing rates of both the average (Lasker et al., 2008) and individual (Park et al., 2010) regular and irregular afferent by filtering the head movement traces using the estimated transfer function parameter values (see Table 4 of Lasker et al., 2008). The continuous-time transfer functions, given in terms of their Laplace transforms, were converted to digital filter coefficients by first applying the bilinear transform to the integral of the transfer function (i.e. neglecting the zero at t=0). The head movement traces were filtered in software

using these resulting filter coefficients, and then differentiated by taking the difference between each consecutive sample (i.e. omitting the zero at t=0). The head movement traces were then filtered in software using these resulting filter coefficients and differentiated in the time domain to yield an estimate of the instantaneous firing rate.

Simulation of afferent fiber spike trains

Spike trains from the average and individual regular and irregular afferents in response to the recorded head movement traces were simulated probabilistically using the instantaneous firing rate derived from the transfer function above (with negative rates set to zero). Additionally, the variability in spike timing was modeled based on the average normalized coefficient of variation for each afferent type. Spike trains were modeled as an inhomogeneous gamma process (Berman, 1981) with shape parameter $K = \frac{1}{CV*^2}$, as follows:

The instantaneous firing rate traces, estimated from afferent transfer functions, were first upsampled to 5 KHz by interpolation. Then, at each sample time, the number of spikes occurring between that sample and the next was drawn randomly from a Poisson distribution with rate parameter:

$$\lambda[n_{up}] = K \cdot dr[n_{up}]/Fs_{up}$$

Where λ is the Poisson rate, K is the shape parameter as described above rounded to the nearest integer, dr is the instantaneous firing rate, n_{up} is the interpolated sample number, and Fs_{up} is the upsampled rate (5kHz). The resulting instantiation of the Poisson process was then transformed to a Gamma process by selecting only every K^{th} spike to form the model spike train with rate function dr. For a constant firing rate (i.e. homogeneous Gamma process), this method produces a spike train with Gamma distributed interspike intervals with $CV = 1/\sqrt{K}$.

Supplemental References

Berman, M. (1981). Inhomogenous and modulated gamma processes. Biometrika, 68: 143-152.

Lasker, D. M., Han, G. C., Park, H. J., and Minor, L. B. (2008). Rotational responses of vestibular-nerve afferents innervating the semicircular canals in the C57BL/6 mouse. J Assoc Res Otolaryngol *9*, 334-348.

Park, H. J., Lasker, D. M., and Minor, L. B. (2008). Static and dynamic discharge properties of vestibular-nerve afferents in the mouse are affected by core body temperature. Experimental Brain Research *200*, 269-275.